Molecular Crystals and Liquid Crystals Science and Technology. Section A. Molecular Crystals and Liquid Crystals
Publication details, including instructions for authors and subscription information:
http://www.tandfonline.com/loi/gmcl19

# X-Ray-Excited Photocurrent in Anthracene Crystals

J. Godlewski [a] , R. Signerski [a] , J. Kalinowski [b] , S. Stizza [c] & M. Berretoni [c]

[a] Department of Molecular Physics, Technical University of Gdańsk, 80-952, Gdańsk, Poland

[b] Istituto di Fotochimica e Radiazioni d'Alta Energia, 40126, Bologna, Italy

[c] Dipartimento di Matematica e Fisica, Universita di Camerino, 60123, Camerino, Italy

Version of record first published: 24 Sep 2006.

To cite this article: J. Godlewski , R. Signerski , J. Kalinowski , S. Stizza & M. Berretoni (1994): X-Ray-Excited Photocurrent in Anthracene Crystals, Molecular Crystals and Liquid Crystals Science and Technology. Section A. Molecular Crystals and Liquid Crystals, 252:1, 145-154

To link to this article: http://dx.doi.org/10.1080/10587259408038220

*Mol. Cryst. Liq. Cryst.* 1994, Vol. 252, pp. 145–154
Reprints available directly from the publisher
Photocopying permitted by license only

Printed in the United States of America



# X-RAY-EXCITED PHOTOCURRENT IN ANTHRACENE CRYSTALS

J. GODLEWSKI[*], R. SIGNERSKI[*], J. KALINOWSKI[**], S. STIZZA[***] and M. BERRETONI[***]

[*] Department of Molecular Physics, Technical University of Gdańsk. 80-952 Gdańsk, Poland,

[**] Istituto di Fotochimica e Radiazioni d'Alta Energia, 40126 Bologna, Italy,

[***] Dipartimento di Matematica e Fisica, Universita di Camerino, 60123 Camerino, Italy.

Abstract The mechanism of charge carrier generation by X-rays in anthracene crystals has been studied. We conclude that charge carrier pairs are generated by electrons due to the scattering of X-rays and the separation mechanism is in disagreement with the Onsager model. Recombination of charge carriers determines the slope of the photocurrent-electric field characteristics. The experimental current-electric field characteristics have been described theoretically and the role of photoinjection of charge carriers by X-rays from metallic electrodes has been established.

*Keywords: X-ray, photocurrent, organic crystal, anthracene, charge generation, charge separation*

## 1. INTRODUCTION

The mechanism of charge carrier generation by X-rays in anthracene crystals has been studied and described by several authors [1,2,3]. Basic experimental results were obtained with a flash X-ray system with full lamp spectrum and relatively thick anthracene crystals. The experimental results obtained give inconsistent information about mechanisms of charge carrier generation in anthracene crystals. Hughes [3] postulates, that charge carrier separation is due to the Onsager model [4]. Kepler and Coppage [1] have demonstrated that the amount of generated charge carriers is independent of temperature, which contradicts the Onsager model [4,5]. Consequently, we feel that the mechanism of generation and separation of the charge carriers produced by X-rays still remains an open question.

The purpose of this paper is an analysis of mechanism of charge carrier generation and of charge carrier separation in anthracene crystals illuminated by X-rays.

## 2. EXPERIMENTAL RESULTS

The paper presents experimental data on the conductivity generated by X-ray photons obtained from the Rigaku System for EXAFS measurements. Thin anthracene crystals (of about 100 μm) with metallic electrodes evaporated in a sandwich arrangement were investigated. The experimental data are focused on photocurrent-electric field characteristics, the efficiency of volume charge carriers generation, and photoinjection of charge carriers from metallic electrodes into the anthracene crystals.

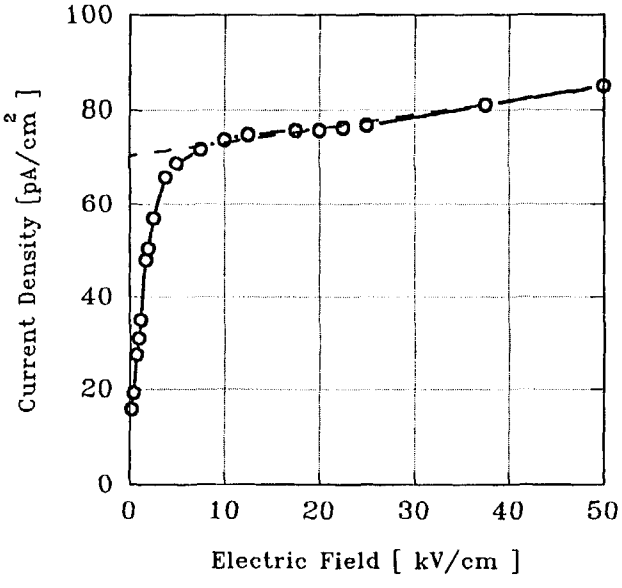


FIGURE 1. Photocurrent-electric field relationship for a 40μm-thick anthracene crystal obtained by illumination with X-rays at the energy E=8.4keV. The crystal sandwiched between two vacuum-evaporated gold electrodes. Solid line-experiment; dashed line-linear extrapolation to F=0.

The current-electric field characteristics were obtained with monochromatic X-rays or a full spectrum of the tungsten lamp. The volume efficiency of charge carrier generation, defined as $j/eI_0$, has been measured versus photon energy and an estimation of the role of electrode charge injection by X-rays in the charge production has been undertaken.

The current-electric field relationship for a monochromatic line with energy W = 8.4 keV is shown in fig.1. The initial steep increase in the current is followed by a weakly varying function of the electric field. The photogeneration yield is practically independent of photon energy as shown in fig. 2. Its value of about 2 means that an X-ray photon can produce four orders of magnitude more electron-hole pairs than a photon from the ultraviolet range [5].

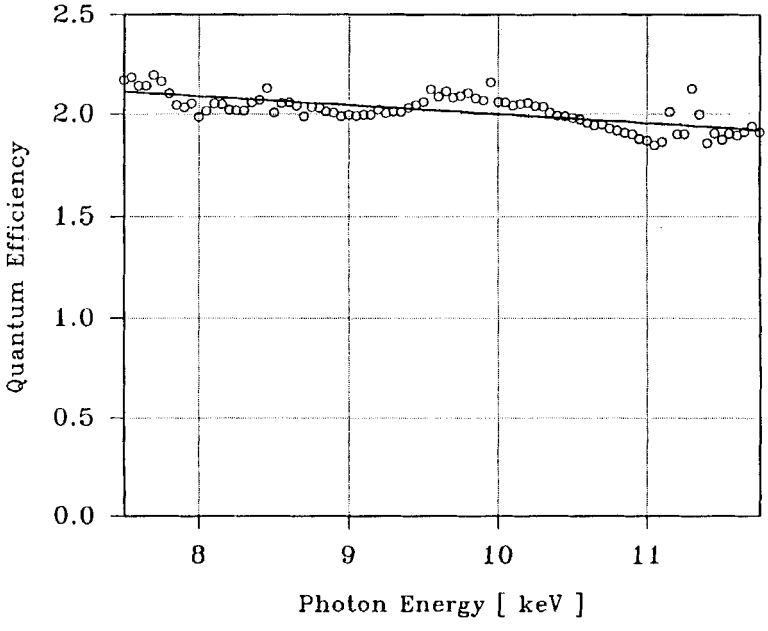


FIGURE 2. Photogeneration effective quantum yield as a function of photon energy for anthracene crystal. Crystal the same as in fig.1. The applied field $F_0=1.25\cdot10^4$V/cm.

For anthracene crystals provided with copper electrodes noticed that at photon energies araund W ≅ 9keV quantum efficiency of charge carrier production increased due to the sharply changing absorption coefficient of copper in this region of energies [6]. The relevant data are presented in fig.3.

The slope-to-intercept ratio of the high-field segment of the current voltage relationship in fig.1 is $3.6\cdot10^{-6}$cm/V.

This is an order of magnitude smaller than theoretical value $3.6\cdot10^{-5}$cm/V [5] resulting from Onsager model. The difference exceeds

the posible experimental error and therefore further experimental data current-electric field characteristics seemed necessary. The current field plots obtained with the full spectrum of the X-ray lamp are shown in fig.4. The values of the slope-to-intercept ratio equal $0.8 \cdot 10^{-5}$cm/V (a), $1.2 \cdot 10^{-5}$cm/V (b) and $1.8 \cdot 10^{-5}$cm/V (c) are again different from those calculated on the basis of the Onsager model, and vary with the level of excitation.

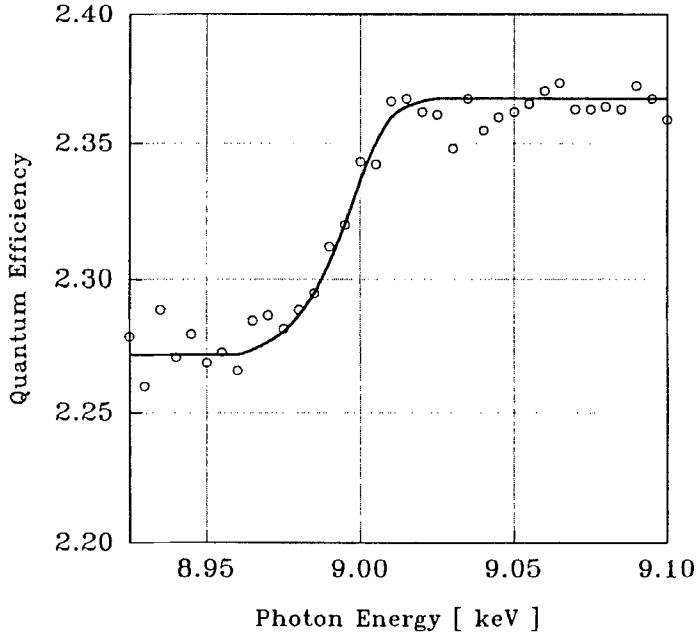


FIGURE 3. Effective quantum efficiency of photocurrent in anthracene crystals as a function of photon energy with present the photoinjection from copper electrode near $K_\alpha$ line of copper. Thickness of the crystal d = 120 μm, electric field applied $10^4$ V/cm.

We conclude that the Onsager model cannot be used to describe the current-field relationship for to the photogeneration of charge carrier by a steady state X-rays flux in anthracene crystals, because the experimental value of the slope-to-intercept ratio is a function of excitation level and falls below the value calculated from the model.

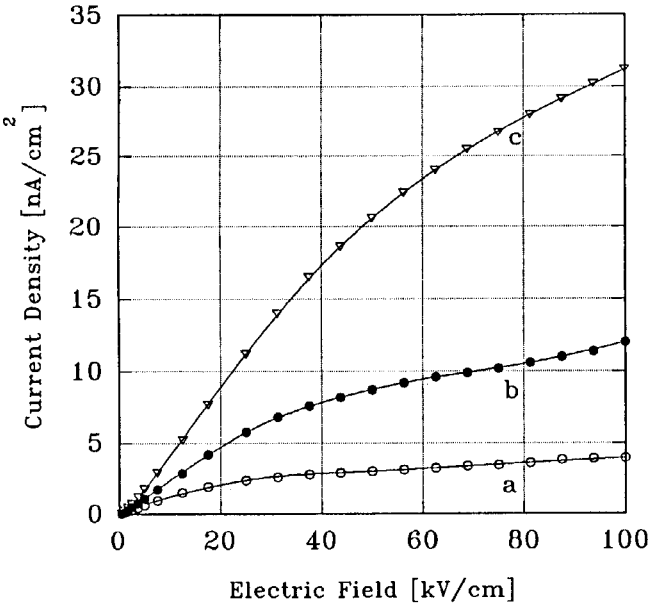


FIGURE 4. Photocurrent-electric field characteristics for X-ray generated charge carriers in anthracene crystal with using total spectrum of tungsten lamp, lamp voltage U = 15 kV and lamp current 10 mA (a), 30 mA (b) and 100 mA (c). Crystal the same as in fig. 1.

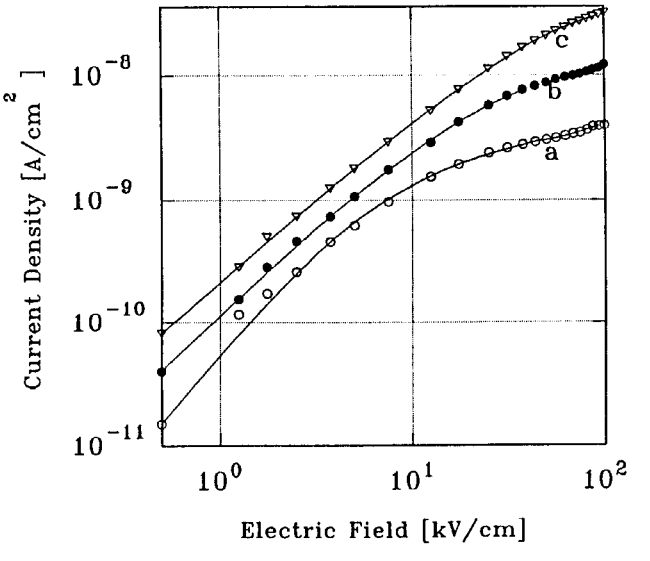


FIGURE 5. Experimental data from fig. 4 redrawn in double logarithmic scale. Explanation in the text.

## 3. THEORETICAL MODEL FOR THE CURRENT-ELECTRIC FIELD DEPENDENCE

To describe the voltage evolution of the photocurrent we consider the continuity and the Poisson equations for steady state conditions:

$$\frac{dp(x)}{dt} = G(F,x) - \alpha\, n_t(x)\, p(x) - \frac{1}{e}\,\frac{dj_p(x)}{dx} = 0 , \tag{1}$$

$$\frac{dn(x)}{dt} = G(F,x) - \alpha\, p_t(x)\, n(x) + \frac{1}{e}\,\frac{dj_n(x)}{dx} = 0 , \tag{2}$$

$$j_p(x) = p(x)\, e\, \mu_p\, F(x) , \tag{3}$$

$$j_n(x) = n(x)\, e\, \mu_n\, F(x) , \tag{4}$$

$$j = j_n(x) + j_p(x) , \tag{5}$$

$$\frac{dF(x)}{dx} = \frac{e}{\varepsilon\,\varepsilon_0}\left[\, p_t(x) - n_t(x) \,\right] , \tag{6}$$

$$n_t(x)\,\Theta = n(x),\quad p_t(x)\,\Theta = p(x) . \tag{7}$$

Here $n(x)$ and $p(x)$ are concentrations of free electrons and holes, respectively, as functions of distance from the electrode $x$; $n_t(x)$, $p_t(x)$ are concentrations of trapped electrons and holes; $G(F,x)$ is generation term, which can be a function of the electric field $F$; $\alpha$ is recombination rate; $j_n(x)$ and $j_p(x)$ are electron and hole currents, respectively; $\mu_n$ and $\mu_p$ are mobilities of electrons and holes, respectively; $j$ is the total current; $\varepsilon_0$ and $\varepsilon$ are the permitivities of vacuum and the dielectric used; and $\Theta$ is a parameter describing the relation between the concentrations of free and trapped charge carriers.

In the above equations it is assumed that the concentrations $n \ll n_t$ and $p \ll p_t$. For a discussion of the experimental data concerning the photogeneration of charge carriers by X-rays in anthracene crystals, it is necessary to make some assumptions. Further analysis will be made with the assumptions that generation rate is practically independent of the distance from the electrode and of the electric

field ($G(F,x) = G_0$), and that the effective mobility

$$\mu_p \Theta = \mu_n \Theta = \mu_0 \Theta = \mu \tag{8}$$

is independent of the nature of charge carriers.

Consider some limiting cases.

(i) The space charge limited conditions ( $F(0) \longrightarrow 0$) and the following relations to be fulfilled:

$$\left| \frac{1}{e} \frac{dj_p(x)}{dx} \right| << \alpha\, n_t(x)\, p(x) , \tag{9}$$

$$\left| \frac{1}{e} \frac{dj_n(x)}{dx} \right| << \alpha\, p_t(x)\, n(x) , \tag{10}$$

The current-electric field relationship is then given by:

$$j = \left[ \left(1 - \frac{\pi}{4}\right) \frac{\varepsilon\varepsilon_0\mu}{2a^{3/2}} \right]^{-1} \left\{ \frac{d}{2a^{1/2}} - \left[ \frac{d^2}{4a} - \left(1 - \frac{\pi}{4}\right) \frac{\varepsilon\varepsilon_0\mu}{a^{3/2}} U \right]^{1/2} \right\} \tag{11}$$

In the above expression, U is the voltage applied to a sample with thickness d, and

$$a = \left[ \frac{G_0}{\alpha} (e\mu)^2 \right] . \tag{12}$$

Equation (11) is fulfilled for low values of photocurrent, such as

$$j \leq \frac{2ad}{\varepsilon\varepsilon_0\mu} . \tag{13}$$

(ii) The intermediate region between the space charge limited condition and the saturation currents. After using conditions (9) and (10), and assuming that in the middle of the sample:

$$\frac{dF(x)}{dx} = \Big|_{x=d/2} = 0 , \tag{14}$$

but $F(0)$ and $F(d)$ are different from zero, the current-electric field

dependence can be described by the relation

$$\frac{d}{2}\left[\frac{j^2}{4a} - a\left(\frac{d}{\varepsilon\varepsilon_0\mu}\right)^2\right]^{1/2} + \frac{j^2\varepsilon\varepsilon_0\mu}{8a^{3/2}} \arcsin\frac{2ad}{j\varepsilon\varepsilon_0\mu} = U \,. \qquad (15)$$

The above relation describes photocurrent for the region between the space charge limited current and the saturation current.

(iii) The electric field in the sample approximated by $F(x)=F_0\approx\frac{U}{d}$, the current becomes saturated. In this case the general description of the current-electric field characteristics has the form

$$\frac{2(e\ \mu\ F_0)^2}{(4a\ F_0^2 - j^2)^{1/2}}\left[\operatorname{arctg}\frac{j\ (4\pi\ a\ F_0^2 - j^2)^{1/2}}{j^2 + 4a\ F_0^2}\right] = \alpha\ e\ d \,. \qquad (16)$$

From relations (11), (15) and (16) we can find approximate expressions for the current-electric field characteristics in the relevant regions.

For case (i), on the basis of eq. (11), we have:

$$j \cong 2a^{1/2}\ \frac{U}{d}, \quad \text{for} \quad j \le \frac{2ad}{\varepsilon\varepsilon_0\mu} \text{ and } U < \frac{d^2a^{1/2}}{\varepsilon\varepsilon_0\mu} \,, \qquad (17)$$

for case (ii), on the basis of eq. (15), we have:

$$j \cong \frac{4a^{3/4}}{(\pi\varepsilon\varepsilon_0\mu)^{1/2}}\ U^{1/2}, \quad \text{for} \quad \frac{2ad}{\varepsilon\varepsilon_0\mu} \le j \le 2G_0ed \,, \qquad (18)$$

and for case (iii), on the basis of eq. (16), we have:

$$j \cong 2G_0ed, \quad \text{where} \quad G_0 = \varphi I_0\kappa \,, \qquad (19)$$

and where $\varphi$ is the generation quantum yield. It is the maximum value of the photocurrent. $I_0$ is the flux of the incident light permit area and $\kappa$ - linear absorption coefficient. The absorption coefficient is a function of the photon energy [6].

## 4. DISCUSSION

The above theoretical analysis shows that for low electric fields a linear relationship between photocurrent and electric field with the slope dependent on the square root of intensity of incident radiation ($I_0$) applies. From the data in fig.4 for the lower values of electric field, assuming linear increase of the current with electric field the experimental values of a are as follows:

$$a \cong 3.6 \cdot 10^{-23} \left( \frac{A}{V\ m} \right)^2 \qquad \text{(a)},$$

$$a \cong 1.7 \cdot 10^{-22} \left( \frac{A}{V\ m} \right)^2 \qquad \text{(b) and}$$

$$a \cong 6.3 \cdot 10^{-22} \left( \frac{A}{V\ m} \right)^2 \qquad \text{(c)}.$$

These values are correlated with the flux intensity of the X-ray used to obtain the experimental data and theoretical eq.(17).

For the higher values we can expect on the basis of eq.(18), that photocurrent is proportional to the square root of electric field. To demonstrate this relation, fig.5 shows data from fig.4 in a double logarithmic scale. For the lower values of electric field the slope is close to 1,25 and for the higher values it is about 0.5, in agreement with the prediction from eq.(18). For the lower values of electric field the value of slope is greater than one. It can be due to an increase of generation term as a function of electric field.

We can infer from the data presented in fig.2 that quantum efficiency of charge carrier generation is practically independent of energy. This corresponds to the fact that absorption of X-rays by the scattering mechanism is practically independent of energy [6]. This observation confirms earlier discussions of the mechanism of charge carrier generation by secondary electrons in the literature [1,2,3].

Finally we can conclude that charge carrier pairs are generated by electrons due to the scattering of X-rays and the separation mechanism is in disagreement with the Onsager model, as the energy of X-ray generated electrons is sufficient to separate the carriers during the generation event. Another process which controls quantum efficiency of charge carrier generation is bimolecular recombination. Recombination of charge carriers determines the shape of the photocurrent-electric field characteristics. Photoinjection of charge

carriers by X-rays from metallic electrode also contributes to the photocurrent. It can be seen as the step increase of quantum efficiency in fig.3 for energy near the $K_\alpha$ absorption for copper electrode.

ACKNOWLEDGEMENTS

The work was supported by KBN under Program Nr 204599101

LITERATURE

1. R.G.Kepler and F.N.Coppage, Phys. Rev., 151, 610 (1966)
2. W.G.Perkins, J.Chem.Phys., 48, 931 (1968)
3. R.G.Hughes, J.Chem.Phys., 55, 5442 (1971)
4. L.Onsager, Phys.Rev., 54, 554 (1938)
5. R.R.Chance and C.Braun, J.Chem.Phys., 64, 3573 (1976)
6. J.W.Robinson, Ed., "Handbook of Spectroscopy", CNR Press 1974.